

# Peculiarities in the spectrum of coherent emission from relativistic electrons crossing a thin aligned crystal

N. Nasonov , G. Pokhil, P. Zhukova

*Laboratory of Radiation Physics (Lebedev Physical Institute RAS, NPI Moscow Lomonosov University,  
Belgorod State University), 14 Studencheskaya, 308007 Belgorod, Russia*

---

## Abstract

An emission from relativistic electrons crossing an aligned crystal is considered with account of coherent bremsstrahlung on atomic strings and transition radiation contributions. Some peculiarities in the low energy range of the emission spectrum caused by azimuthal scattering of emitting electrons on atomic strings and an interference between the transition radiation and coherent bremsstrahlung are predicted and analyzed theoretically.

---

*Keywords:* Relativistic electron; Coherent bremsstrahlung; Transition radiation; Multiple scattering

---

## 1. Introduction

When a relativistic electron crosses an aligned crystal near parallel to the axis of a set of atomic strings it is scattered coherently by atoms constituting the single string. As a consequence the contribution of string's atoms to bremsstrahlung involved in such a scattering process becomes coherent as well [1]. Characteristics of the coherent bremsstrahlung yield from the total crystal depend

strongly on the correlations between consecutive collisions of the emitting electron with different atomic strings. In case the orientation angle  $\Psi$  between the emitting electron velocity and the string's axis exceeds the critical angle of axial channelling  $\Psi_{ch}$  and the component of such a velocity in the plane normal to this axis is oriented close to conditions of planar channelling the constructive interference between emission amplitudes in different strings can be realized. As this takes place the strong maxima appear in the coherent bremsstrahlung spectral-angular distribution [1,2]. The mentioned constructive interference is destroyed in the range of small orientation angles  $\Psi \sim \Psi_{ch}$

due to essential growth of the emitting particle coherent azimuthal scattering by atomic strings. Under these conditions the coherent bremsstrahlung spectrum is determined by the process of emitting electron interaction with a single string within the range of high enough photon energies  $\omega$ , where the emission formation length  $l_{\text{coh}} \sim 2\gamma^2/\omega$  ( $\gamma$  is the Lorentz factor of emitting electrons) is smaller than the average electron path between consecutive collisions of this electron with atomic strings  $\bar{l}_\perp/\Psi$  ( $\bar{l}_\perp = 1/\sqrt{n_\alpha d}$ ,  $n_\alpha$  is the density of atoms,  $d$  is the distance between neighbouring atoms in the string) [2]. More complicated situation is realized in small photon energy range, where  $l_{\text{coh}} \gg \bar{l}_\perp/\Psi$  and the emission yield is formed in the process of multiple scattering of emitting electrons on atomic strings. It is precisely this photon energy range that is of prime interest for studies of our work.

One of the main new effects appearing in the coherent bremsstrahlung within the discussed frequency range consists in the suppression of dipole emission yield, predicted in [3]. More recently, this effect has been confirmed in work [4], where an agreement of obtained theoretical results with experimental data has been shown as well. It should be noted that only the spectrum of non-collimated emission was studied in [3,4]. In contrast with that we perform a detailed study of both spectral-angular and spectral distributions of dipole coherent bremsstrahlung. In addition to this we take into account the transition radiation contribution and its interference with coherent bremsstrahlung. It will be shown that the inclusion of outlined factors changes very essentially the emission properties.

A further effect of the coherent bremsstrahlung suppression manifests in the range of high emitting electron energies, when the multiple scattering angle achievable on the distance of the order of  $l_{\text{coh}}$  becomes greater than the characteristics emission angle for relativistic particles  $\gamma^{-1}$ . Such a suppression effect analogous to known Landau–Pomeranchuk–Migdal (LPM) effect of the bremsstrahlung suppression due to multiple scattering of emitting particles moving in an amorphous medium has been predicted in [5] and studied in detail in [3] for the specific case of large orientation angles  $\Psi \gg \Psi_{\text{ch}}$  when the angle of emitting electron azi-

muthal scattering on a single atomic string is small and the emission process in a crystal is identical to that in an amorphous medium. Analysis performed in this work shows that LPM effect manifestation in a crystal may be different essentially in the general case from that in an amorphous medium.

The paper is organized as follows. In Section 2 we obtain the general expressions for the total emission spectral-angular distribution, using the general approach based on the summation of elementary emission amplitudes corresponding to interactions of an emitting electron with different atomic strings. Section 3 is devoted to study of the coherent bremsstrahlung contribution to total emission yield. We give an exhaustive description and a correct physical explanation of the mentioned above suppression of the dipole coherent bremsstrahlung. The contribution of transition radiation and its interference with coherent bremsstrahlung is considered in Section 4. Anomalous manifestation of the Ter-Mikaelian effect of the bremsstrahlung dielectric suppression is shown in this section. In Section 5 we study beyond the frame of dipole approximation the suppression of strongly collimated coherent bremsstrahlung, caused by azimuthal multiple scattering of emitting electrons. Analysis of such a suppression effect for non-collimated coherent bremsstrahlung is performed in Section 6. The characteristics of this effect and LPM effect in an amorphous medium are compared in this section. Our conclusions are given in Section 7.

## 2. General expressions

Let us consider an emission from relativistic electrons crossing a crystalline target near the normal  $\mathbf{e}$  to this target surface, so that the velocity of emitting particle  $\mathbf{V}(t)$  and the unit vector to the direction of emitted photon observation  $\mathbf{n}$  can be represented as

$$\mathbf{V}(t) = \mathbf{e} \left( 1 - \frac{1}{2} \gamma^{-2} - \frac{1}{2} \Psi_t^2 \right) + \Psi_t, \quad \mathbf{e} \Psi_t = 0, \quad (1a)$$

$$\mathbf{n} = \mathbf{e} \left( 1 - \frac{1}{2} \Theta^{-2} \right) + \Theta, \quad \mathbf{e} \Theta = 0, \quad (1b)$$

where  $\gamma$  is the Lorentz factor of emitting electron,  $\Psi_t \equiv \Psi(t)$  is the scattering angle of this electron,  $\Psi_i, \Theta \ll 1$ . Taking into account the transition radiation and bremsstrahlung emission mechanisms and using the generally accepted methods of classical electrodynamics [1,6] (we consider the emission process in the small photon energy range  $\omega \ll m\gamma$ ,  $m$  is the electron mass) one can obtain the expression for the total emission amplitude  $\mathbf{A}_n$  in the very convenient for further analysis from [7]

$$\begin{aligned} \mathbf{A}_n = & \frac{e}{\pi} \left[ (\Psi_i - \Theta) \left( \frac{1}{\gamma^{-2} + (\Psi_i - \Theta)^2} - \frac{1}{\gamma_*^{-2} + (\Psi_i - \Theta)^2} \right) \right. \\ & - (\Psi_f - \Theta) \left( \frac{1}{\gamma^{-2} + (\Psi_f - \Theta)^2} - \frac{1}{\gamma_*^{-2} + (\Psi_f - \Theta)^2} \right) \\ & \times \exp \left( \frac{i\omega}{2} \int_0^L dt \left( \gamma_*^{-2} + (\Psi_t - \Theta)^2 \right) \right) \\ & - \int_0^L dt \cdot \exp \left( \frac{i\omega}{2} \int_0^t d\tau \left( \gamma_*^{-2} + (\Psi_\tau - \Theta)^2 \right) \right) \\ & \left. \times \left( \frac{d}{dt} \frac{\Psi_t - \Theta}{\gamma_*^{-2} + (\Psi_t - \Theta)^2} \right) \right], \quad (2) \end{aligned}$$

where  $\Psi_i$  and  $\Psi_f$  are the initial and final values of  $\Psi_t$  respectively,  $L$  is the thickness of the target,  $\gamma_*^{-2} = \gamma^{-2} + \omega_p^2/\omega^2$ ,  $\omega_p$  is the target's plasma frequency.

As is easy to see, the first and second terms in the expression (2) describe the transition radiation from in and out surfaces of the target. These terms vanish without account of the target's dielectric susceptibility  $\chi(\omega) = -\omega_p^2/\omega^2$ . The last term on (2) corresponds to bremsstrahlung contribution. This term vanishes for the particle moving with a constant velocity.

It should be noted that the target's atomic structure is not fixed in the expression (2). Earlier this expression was used for the analysis of the relativistic electron bremsstrahlung in amorphous target [7]. In this work we consider the coherent bremsstrahlung on a set of atomic strings placed in the crystalline target parallel to the normal  $\mathbf{e}$ , so that the scattering angle  $\Psi_t$  is simultaneously the orientation angle of the emitting particle velocity  $\mathbf{V}(t)$  relative to the string's axis.

Since the emitting electron velocity  $\mathbf{V}(t)$  can be changed essentially during small time intervals only, corresponding to collisions of this electron

with atomic strings, one can represent the total emission amplitude (2) as a sum of elementary amplitudes describing the emission on different strings. Within the small frequency range

$$\frac{\omega R}{2\gamma_*^2 \Psi} \ll 1, \quad (3)$$

when the emission formation length  $l_{coh}$  exceeds essentially the effective electron path in a string's potential  $R/\Psi$  ( $R$  is the screening radius in Fermi–Thomas atom model,  $R$  determines the effective transverse size of an atomic string) and, as a consequence, the emission, appearing in  $k$ th collision of the emitting electron with a single atomic string, is determined by the scattering angle  $\Psi_{k+1} - \Psi_k$  only ( $\Psi_{k+1}$  and  $\Psi_k$  are the values of the angle  $\Psi(t)$  after and before  $k$ th collision respectively) the total amplitude (2) reduces to

$$\begin{aligned} \mathbf{A}_n = & \frac{e}{\pi} \left[ (\Psi_i - \Theta) \left( \frac{1}{\gamma^{-2} + (\Psi_i - \Theta)^2} - \frac{1}{\gamma_*^{-2} + (\Psi_i - \Theta)^2} \right) \right. \\ & - (\Psi_f - \Theta) \left( \frac{1}{\gamma^{-2} + (\Psi_f - \Theta)^2} - \frac{1}{\gamma_*^{-2} + (\Psi_f - \Theta)^2} \right) \\ & \times \exp \left( \frac{i\omega}{2} \sum_k \left( \gamma_*^{-2} + (\Psi_k - \Theta)^2 \right) \tau_k \right) \\ & - \sum_k \left( \frac{\Psi_k - \Theta}{\gamma_*^{-2} + (\Psi_k - \Theta)^2} - \frac{\Psi_{k-1} - \Theta}{\gamma_*^{-2} + (\Psi_{k-1} - \Theta)^2} \right) \\ & \left. \times \exp \left( \frac{i\omega}{2} \sum_{j \leq k} \left( \gamma_*^{-2} + (\Psi_j - \Theta)^2 \right) \tau_j \right) \right], \quad (4) \end{aligned}$$

where  $\tau_k$  is the interval between  $k-1$ th and  $k$ th collisions.

The following from (4) expression for spectral-angular distribution

$$\begin{aligned} \omega \frac{dN}{d\omega d^2\Theta} = & \langle |\mathbf{A}_n|^2 \rangle \\ = & \omega \frac{dN^{cb}}{d\omega d^2\Theta} + \omega \frac{dN^{tr}}{d\omega d^2\Theta} + \omega \frac{dN^{int}}{d\omega d^2\Theta}, \quad (5) \end{aligned}$$

takes into account, among contributions of coherent bremsstrahlung (the first term in (5)) and transition radiation (the second term), an interference between these emission mechanisms. The brackets  $\langle \rangle$  in (5) mean the averaging over accidental variables  $\Psi_k$  and  $\tau_k$ .

### 3. Contribution of the dipole coherent bremsstrahlung

Let us consider the coherent bremsstrahlung contribution using the general expressions (4) and (5). The most general formula for the coherent bremsstrahlung spectral-angular distribution has the form

$$\begin{aligned} \omega \frac{dN^{cb}}{d\omega d^2\Theta} &= \frac{e^2}{\pi^2} \\ &\times \sum_k \left\langle \left( \frac{\Psi_k - \Theta}{\gamma_*^{-2} + (\Psi_k - \Theta)^2} - \frac{\Psi_{k-1} - \Theta}{\gamma_*^{-2} + (\Psi_{k-1} - \Theta)^2} \right)^2 \right. \\ &+ 2\text{Re} \sum_{m \geq 1} \left( \frac{\Psi_k - \Theta}{\gamma_*^{-2} + (\Psi_k - \Theta)^2} - \frac{\Psi_{k-1} - \Theta}{\gamma_*^{-2} + (\Psi_{k-1} - \Theta)^2} \right) \\ &\times \left( \frac{\Psi_{k+m} - \Theta}{\gamma_*^{-2} + (\Psi_{k+m} - \Theta)^2} - \frac{\Psi_{k+m-1} - \Theta}{\gamma_*^{-2} + (\Psi_{k+m-1} - \Theta)^2} \right) \\ &\times \exp \left( \frac{i\omega}{2} \sum_{p=1}^m (\gamma_*^{-2} + (\Psi_{k+p} - \Theta)^2) \tau_{mp} \right) \Bigg\rangle. \quad (6) \end{aligned}$$

Averaging of the expression (6) is very complicated task in the general case (we will perform such averaging in the specific case of strongly collimated emission). Here we restrict our consideration to the case of small enough scattering angles, when the condition of the dipole approximation in the relativistic particle emission theory

$$\gamma^2 \langle (\Delta\Psi_{coh})^2 \rangle \ll 1, \quad (7)$$

is valid,  $\Delta\Psi_{coh}$  is the scattering angle achievable on the distance of the order of the emission formation length  $l_{coh}$ .

Performing the necessary expansions by the use of (7) we can reduce the general expression (6) to more simple one

$$\begin{aligned} \omega \frac{dN^{cb}}{d\omega d^2\Theta} &= \frac{e^2}{\pi^2} \frac{1}{(\gamma_*^{-2} + \tilde{\Theta}^2)^2} \sum_k \left\langle (\Psi_k - \Psi_{k-1})^2 \right. \\ &- \frac{4\gamma_*^{-2}}{(\gamma_*^{-2} + \tilde{\Theta}^2)^2} (\tilde{\Theta}, \Psi_k - \Psi_{k-1})^2 \\ &+ 2\text{Re} \sum_{m \geq 1} \left[ (\Psi_k - \Psi_{k-1}, \Psi_{k+m} - \Psi_{k+m-1}) \right. \\ &- \frac{4\gamma_*^{-2}}{(\gamma_*^{-2} + \tilde{\Theta}^2)^2} (\tilde{\Theta}, \Psi_k - \Psi_{k-1})(\tilde{\Theta}, \Psi_{k+m} - \Psi_{k+m-1}) \\ &\times \exp \left( \frac{i\omega}{2} (\gamma_*^{-2} + \tilde{\Theta}^2) \sum_{p=1}^m \tau_{k+p} \right) \Bigg\rangle, \quad (8) \end{aligned}$$

where  $\tilde{\Theta} = \Theta - \Psi_i$ .

Averaging over  $\tau_k$  in (8) is performed with account of independence of different accidental quantities  $\tau_k$ . Using the distribution function [8]  $f(\tau) = (1/\bar{\tau}) \exp(-\tau/\bar{\tau})$ ,  $\bar{\tau} = \bar{l}_\perp / \Psi$ , one can obtain the formula

$$\begin{aligned} &\left\langle \exp \left( \frac{i\omega}{2} (\gamma_*^{-2} + \tilde{\Theta}^2) \sum_{j=1}^k \tau_j \right) \right\rangle \\ &= \left( 1 - \frac{i\omega}{2} \bar{\tau} (\gamma_*^{-2} + \tilde{\Theta}^2) \right)^{-k}. \quad (9) \end{aligned}$$

When averaging over  $\Psi_k$  in (8) one should take into account the unique property of electron coherent scattering by the average potential of atomic string consisting in the conservation law:  $\Psi_k^2 = \Psi_{k+1}^2$ . It is well known that only azimuthal angle  $\chi$  of the vector  $\Psi$ , is changed due to electron collision with atomic string. Therefore

$$\Psi_k = \Psi(\mathbf{e}_x \cos \chi_k + \mathbf{e}_y \sin \chi_k), \quad \chi_k = \chi_i + \sum_{j \leq k} \Delta \chi_j, \quad (10)$$

where  $\chi_i$  is the initial value of  $\chi$ ,  $\Delta \chi_j$  is the change of azimuthal angle  $\chi$  in  $j$ th collision, it is clear that all  $\Delta \chi_j$  are independent accidental quantities. To average the expression (8) over  $\Delta \chi_j$  one should use the following formula:

$$\begin{aligned} \langle \cos \chi_k \rangle &= \langle \cos \Delta \chi \rangle^k \cdot \cos \chi_i, \quad \langle \sin \chi_k \rangle = 0, \\ \langle \cos \Delta \chi \rangle &= \frac{2}{l_\perp} \int_0^\infty db \cos(\Delta \chi(b)), \\ \Delta \chi &= \pi - 2b \int_{\rho_0}^\infty \frac{d\rho}{\rho^2 \sqrt{1 - \frac{b^2}{\rho^2} + \frac{\Psi_{ch}^2}{\Psi^2} f(\rho)}}, \quad (11) \end{aligned}$$

where  $1 - \frac{b^2}{\rho_0^2} + \frac{\Psi_{ch}^2}{\Psi^2} f(\rho_0) = 0$ ,  $b$  is the impact parameter of electron collision with a string, the string potential is defined as  $\varphi(\rho) = \varphi_0 f(\rho)$ ,  $f(0) = 1$ ,  $\Psi_{ch}^2 = \frac{2e\varphi_0}{m\gamma}$ .

The expression for  $\langle \cos \Delta \chi \rangle$  in (11) shows clearly that only above-barrier electrons are taken into account in the context of our approach. Ignoring of a contribution from the side of channelling electrons to studied emission yield is justified by the small value of this contribution within the frequency range (3) under consideration. Indeed, the spectrum of channelling radiation is mainly

concentrated in the range  $\omega \geq 2\gamma^2 \Psi_{\text{ch}}/R$  [2]. The yield of channelling radiation photons with energies  $\omega \ll 2\gamma^2 \Psi_{\text{ch}}/R$  is strongly suppressed due to periodicity of channelling particle trajectories, because  $\mathbf{E}_\omega \sim W_\omega \rightarrow 0$  if  $\omega \rightarrow 0$  for the trajectories with  $\langle \mathbf{W}(t) \rangle = 0$  ( $\mathbf{E}_\omega$  and  $\mathbf{W}_\omega$  are the Fourier-transforms of the emission electrical field  $E(\mathbf{r}, t)$  and emitting electron acceleration  $\mathbf{W}(t)$ ).

Using (9)–(11) one can perform the averaging of the expression (8) and obtain the following result:

$$\begin{aligned} \omega \frac{dN^{\text{cb}}}{d\omega d^2\tilde{\Theta}} &= \frac{2e^2 \Psi^2}{\pi^2} \frac{\gamma_*^{-4} + \tilde{\Theta}^4}{(\gamma_*^{-2} + \tilde{\Theta}^2)^4} \\ &\times \left\{ (1 - \langle \cos \Delta\chi \rangle) \frac{\omega^2}{\omega^2 + \omega_*^2(\tilde{\Theta})} \frac{L}{\bar{\tau}} - \frac{\gamma_*^{-2}(\tilde{\Theta}_x^2 - \tilde{\Theta}_y^2)}{\gamma_*^{-4} + \tilde{\Theta}^4} \right. \\ &\times \left[ 1 - \langle \cos \Delta\chi \rangle - (\langle \cos \Delta\chi \rangle \right. \\ &\quad \left. - \langle \cos 2\Delta\chi \rangle) \frac{\omega^2 - \omega_*^2(\tilde{\Theta})}{\omega^2 + \omega_*^2(\tilde{\Theta})} \right] \cdot \frac{1 - \langle \cos 2\Delta\chi \rangle^{\frac{L}{\bar{\tau}}}}{1 - \langle \cos 2\Delta\chi \rangle} \left. \right\}, \end{aligned} \quad (12)$$

where the quantity  $\omega_*(\tilde{\Theta})$  is defined by the formula

$$\omega_*(\tilde{\Theta}) = \frac{2}{\bar{\tau}} \frac{1 - \langle \cos \Delta\chi \rangle}{\gamma_*^{-2} + \tilde{\Theta}^2} \equiv \omega \frac{1 - \langle \cos \Delta\chi \rangle}{\bar{\tau}} l_{\text{coh}}. \quad (13)$$

The important formula (7), determining the fields of applications of the result (12), can be rewritten as

$$\begin{aligned} \gamma^2 \langle (\Delta\Psi_{\text{coh}})^2 \rangle &= 2\gamma^2 \Psi^2 \left[ 1 - \langle \cos \Delta\chi \rangle^{\frac{l_{\text{coh}}}{\bar{\tau}}} \right] \\ &\approx 2\gamma^2 \Psi^2 \left[ 1 - \exp \left( -\frac{1 - \langle \cos \Delta\chi \rangle}{\bar{\tau}} l_{\text{coh}} \right) \right] \\ &\ll 1. \end{aligned} \quad (14)$$

Let us analyze the result (12). It should be noted that the coherent bremsstrahlung yield is described in the main by the first term in (12) proportional to  $\langle k \rangle = L/\bar{\tau}$  on condition  $\langle k \rangle \gg 1$  under consideration ( $\langle k \rangle$  is the average value of total number of emitting electron collisions with atomic strings). Two effects are responsible for the emission yield suppression in small frequency range, as is evident from (12). The well known Ter-Mikaelian effect of

dielectric suppression [1,9] is manifested within the range  $\omega < \gamma\omega_p$ . More unexpected suppression effect appears in the frequency range  $\omega < \omega_*(\tilde{\Theta})$  (the condition  $\omega_*(\tilde{\Theta}) \gg \gamma\omega_p$  must be valid for real observation of this suppression effect).

The nature of this effect consists in a limitation on the emitting electron scattering angle  $\Psi_t$  achievable in the process of coherent azimuthal scattering by atomic strings. To show this (see [4] as well) let us estimate the coherent bremsstrahlung yield on the basis of general expression (2). Since a bremsstrahlung photon is emitted from the section of emitting particle trajectory of length  $l_{\text{coh}}$ , we can estimate the total yield as an incoherent sum of yields from different sections [2]. Neglecting a phase changing in the exponential factor in the bremsstrahlung term in (2) within a single section one can obtain the following estimation:

$$\begin{aligned} \omega \frac{dN^{\text{cb}}}{d\omega d^2\tilde{\Theta}} &\sim \frac{e^2}{\pi^2} \left\langle \left( \frac{\Delta\Psi_{\text{coh}} - \tilde{\Theta}}{\gamma_*^{-2} + (\Delta\Psi_{\text{coh}} - \tilde{\Theta})^2} + \frac{\tilde{\Theta}}{\gamma_*^{-2} + \tilde{\Theta}^2} \right)^2 \right\rangle \frac{L}{l_{\text{coh}}} \\ &\approx \frac{e^2}{\pi^2} \frac{\langle (\Delta\Psi_{\text{coh}})^2 \rangle}{(\gamma_*^{-2} + \tilde{\Theta}^2)^2} \frac{L}{l_{\text{coh}}}, \end{aligned} \quad (15)$$

which is valid within the frame of dipole approximation (14).

It should be noted that the target's atomic structure is not fixed in (15) therefore we can use this formula for estimations of both incoherent bremsstrahlung from amorphous media and coherent bremsstrahlung from crystals. In the former case  $\langle (\Delta\Psi_{\text{coh}})^2 \rangle \sim l_{\text{coh}}$  and the estimation (15) is close to well-known  $\omega$ -independent Bethe–Heitler distribution. In the latter case the quantity  $\langle (\Delta\Psi_{\text{coh}})^2 \rangle$  is given by (14) and the estimation (15) leads to the result

$$\begin{aligned} \omega \frac{dN^{\text{cb}}}{d\omega d^2\tilde{\Theta}} &\sim \frac{2e^2 \Psi^2}{\pi^2} \frac{1 - \langle \cos \Delta\chi \rangle}{(\gamma_*^{-2} + \tilde{\Theta}^2)^2} R \left( \frac{\omega}{\omega_*(\tilde{\Theta})} \right), \\ R &= \frac{\omega}{\omega_*(\tilde{\Theta})} \left( 1 - e^{-\frac{\omega_*(\tilde{\Theta})}{\omega}} \right), \end{aligned} \quad (16)$$

essentially different from Bethe–Heitler one in that the coherent bremsstrahlung yield is suppressed on the range  $\omega < \omega_*(\tilde{\Theta})$  due to the scattering angle

saturation (in accordance with (13), (10) and (14) the inequality  $\omega < \omega_*(\bar{\Theta})$  implies that the emission formation length  $l_{coh}$  exceeds the characteristic distance  $\bar{\tau}/(1 - \langle \cos \Delta\chi \rangle)$ , on which a uniform distribution of emitting electrons over the azimuthal angle  $\chi$  around a string's axis is formed in the process of coherent azimuthal scattering by atomic strings).

Obviously, within the range of high enough emitted photon energies  $\omega \gg \omega_*(\bar{\Theta})$  the estimation (15) coincides with the exact result (12) with an accuracy of a factor  $(\gamma_*^{-4} + \bar{\Theta}^4)/(\gamma_*^{-2} + \bar{\Theta}^2)^2 \approx 1$ . On the other hand the function  $R(\omega/\omega_*(\bar{\Theta}))$  in (16), describing the discussed suppression effect, differs very essentially from  $R_{exact} = (1 + \omega_*^2(\bar{\Theta})/\omega^2)^{-1}$ , following from the exact solution (12). Indeed,  $R \sim \omega/\omega_*(\bar{\Theta})$  for small arguments of this function, whereas  $R_{exact} \sim \omega^2/\omega_*^2(\bar{\Theta})$ . This strong discrepancy is due to an interference between contributions to emission yield from different sections of an emitting particle trajectory, neglected when deriving the simple formula (15). An influence of such interference, essential for the emission of a single photon with fixed energy  $\omega$  and observation angle  $\Theta$ , decreases due to effective averaging over photon phases in the case of a measurement of the total emission spectrum. Integrating (12) over  $\bar{\Theta}$  one can obtain the following result:

$$\begin{aligned} \omega \frac{dN_\psi^{cb}}{d\omega} &= \frac{2e^2}{\pi} \gamma_*^2 \Psi^2 (1 - \langle \cos \Delta\chi \rangle) \cdot \frac{L}{\bar{\tau}} P\left(\frac{\omega}{\omega_0}\right), \\ P &= \frac{\omega}{\omega_0} \left(1 - 2 \frac{\omega^2}{\omega_0^2}\right) \arctan\left(\frac{\omega_0}{\omega}\right) \\ &+ 2 \frac{\omega^2}{\omega_0^2} \left(1 - \ln \sqrt{1 + \frac{\omega_0^2}{\omega^2}}\right), \end{aligned} \quad (17)$$

where  $\omega_0 = \frac{2}{\bar{\tau}} \gamma_*^2 (1 - \langle \cos \Delta\chi \rangle) \equiv \omega_*(0)$ .

The function  $P(\omega/\omega_0)$  behavior is close to  $R(\omega/\omega_*(\bar{\Theta}))$  in (16), as it follows from asymptotes

$$P\left(\frac{\omega}{\omega_0}\right) = \begin{cases} \frac{\pi}{2} \frac{\omega}{\omega_0} & \text{if } \omega \ll \omega_0, \\ \frac{2}{3} & \text{if } \omega \gg \omega_0, \end{cases} \quad (18)$$

suggesting that the interference between contributions to the emission yield from different sections of an emitting particle trajectory is really suppressed for the total emission spectrum.

The result (17) allows to analyze the very important for experiment orientational dependence of the spectrum  $\omega dN^{cb}/d\omega$  on the orientation angle  $\Psi$ . First of all let us consider such a dependence in two limiting cases of large and small values of  $\Psi$  relative to the channelling angle  $\Psi_{ch}$ . In the case of  $\Psi \gg \Psi_{ch}$  the azimuthal scattering angle  $\Delta\chi \sim \Psi_{ch}^2/\Psi^2 \ll 1$  in accordance with (11). As this takes place, the amplitude of the coherent bremsstrahlung spectral distribution decreases proportional to  $\Psi^{-1}$  as it follows from (17). Since  $\omega_0 \sim \Psi^{-3}$  in the range  $\Psi \gg \Psi_{ch}$ , the photon energy region  $\omega < \omega_0$ , where the discussed suppression effect appears, is cut down when increasing of  $\Psi$ .

On the other hand,  $1 - \langle \cos \Delta\chi \rangle \sim 1$  in the range  $\Psi \ll \Psi_{ch}$ . As a consequence, the spectrum (17) decreases proportional to  $\Psi^3$  and the critical energy  $\omega_0$  decreases proportional to  $\Psi$  when decreasing of  $\Psi$  within the range  $\Psi \ll \Psi_{ch}$  under consideration. Thus, the value of the orientation angle  $\Psi \approx \Psi_{ch}$  is best suited to the discussed suppression effect observation. The orientation dependence of the coherent bremsstrahlung spectrum is illustrated in Fig. 1 by the curves calculated by (17) and (11) for different values of the parameter  $\Psi/\Psi_{ch}$ . In accordance with presented curves the most intensive coherent bremsstrahlung from

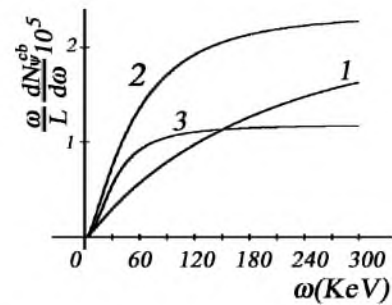


Fig. 1. The orientation dependence of the coherent bremsstrahlung spectrum. The quantity  $\frac{\omega}{L} \frac{dN_\psi^{cb}}{d\omega}$  is presented here by the curves calculated by (17) for Si(110), the energy of emitting electrons  $\epsilon = 500$  MeV. The curves 1, 2, 3 correspond to the ratio  $\Psi/\Psi_{ch} = 0.5, 1, 3$ , respectively.

above-barrier electrons is realized for the orientation angle  $\Psi$  close to the channelling angle  $\Psi_{\text{ch}}$ .

The curves presented in Fig. 1 show a possibility to produce intensive X-rays on the basis of coherent bremsstrahlung from above-barrier electrons. Using (17) and high photon energy limit for the function  $P(\omega/\omega_0)$  in (18), one can obtain the following estimation for the coherent bremsstrahlung spectral density to Bethe–Heitler density ratio:

$$\frac{dN_{\Psi}^{\text{cb}}}{d\omega} / \frac{dN^{\text{BH}}}{d\omega} = \frac{2\Psi^2(1 - \langle \cos \Delta\chi \rangle)}{\Psi_{\text{sc}}^2 \bar{\tau}}, \quad (19)$$

where  $\Psi_{\text{sc}}^2 = \gamma^{-2} L_{\text{sc}}^{-1}$ ,  $L_{\text{sc}} = \frac{e^2}{4\pi} L_{\text{R}}$ ,  $L_{\text{R}}$  is the radiation length,  $\Psi_{\text{sc}}$  is the multiple scattering angle in amorphous medium per unit length. As one would expect, on condition of dipole approximation under consideration the discussed ratio is equal to the ratio between mean squares of emitting electron scattering angles achieved at the same distance in a crystal and in a amorphous medium. This ratio can be much more than unit [2]. The possibility to achieve the value of the ratio (19) of the order of 10 has been demonstrated experimentally in work [10], where an advantage of the discussed emission mechanism over transition radiation has been shown as well.

In the experiment [10] incident electron beam was oriented along the axis of atomic strings. In this case the beam gains at the crystal entry an additional angular spread of the order of  $\Psi_{\text{ch}}$  due to the action from the side of average potential of atomic strings. In addition to this the electron beam distribution over orientation angles  $\Psi$  is changed due to incoherent scattering processes. Assuming that the crystal thickness exceeds essentially the dechannelling length (under these conditions the most part of electrons in the beam are above-barrier [2]) we will use the simplest distribution function

$$f(t, \Psi) = \frac{1}{\pi(\Psi_0^2 + \Psi_{\text{sc}}^2 t)} \exp \left[ -\frac{\Psi^2}{\Psi_0^2 + \Psi_{\text{sc}}^2 t} \right], \quad (20)$$

where  $\Psi_0$  is the initial angular spread of the beam.

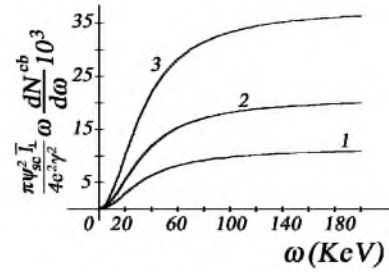


Fig. 2. Influence of the multiple scattering on the coherent bremsstrahlung spectrum. The quantity  $\frac{\pi \Psi_{\text{sc}}^2 I_{\perp}}{4e^2 \gamma^2} \omega \frac{dN^{\text{cb}}}{d\omega}$  is presented here. The curves have been calculated by (21) for Si(110),  $\epsilon = 500$  MeV values of the parameter  $\Psi_{\text{sc}}^2 L = 3$  (curve 1), 5 (curve 2) and 10 (curve 3).

Using (17) and (20) one can obtain the following expression for the coherent bremsstrahlung spectrum in the low frequency range:

$$\begin{aligned} \omega \frac{dN^{\text{cb}}}{d\omega} &= \frac{4e^2 \gamma_*^2}{\pi \Psi_{\text{sc}}^2 I_{\perp}} \int_0^\infty d\Psi \Psi^4 (1 - \langle \cos \Delta\chi \rangle) P\left(\frac{\omega}{\omega_0}\right) \\ &\times \left[ E_1\left(\frac{\Psi^2}{\Psi_0^2 + \Psi_{\text{sc}}^2 L}\right) - E_1\left(\frac{\Psi^2}{\Psi_0^2}\right) \right], \quad (21) \end{aligned}$$

which allows to estimate the maximum possibilities of a possible X-ray source some spectral distributions calculated by (21) are presented in Fig. 2.

It should be noted that the result (21) can not be used for a comparison with the experimental result [10], where a strongly collimated emission yield was measured. Such a comparison we will perform later on the basis of the exact expression for the emission spectral-angular distribution (6).

#### 4. Transition radiation contribution. Influence of an interference between coherent bremsstrahlung and transition radiation

Let us consider now the transition radiation contribution to total emission yield. Starting from the general expression for the total emission amplitude (4) one can obtain the following expression:

$$\begin{aligned} \omega \frac{dN^{\text{tr}}}{d\omega d^2\Theta} &= \frac{e^2}{\pi^2} \left[ (\Psi_i - \Theta)^2 \left( \frac{1}{\gamma^{-2} + (\Psi_i - \Theta)^2} - \frac{1}{\gamma_*^{-2} + (\Psi_i - \Theta)^2} \right)^2 \right. \\ &\quad + \left. \left\langle (\Psi_f - \Theta)^2 \left( \frac{1}{\gamma^{-2} + (\Psi_f - \Theta)^2} - \frac{1}{\gamma_*^{-2} + (\Psi_f - \Theta)^2} \right)^2 \right\rangle \right. \\ &\quad - 2 \left( \frac{1}{\gamma^{-2} + (\Psi_i - \Theta)^2} - \frac{1}{\gamma_*^{-2} + (\Psi_i - \Theta)^2} \right) \\ &\quad \times \text{Re} \left\langle (\Psi_i - \Theta, \Psi_f - \Theta) \right. \\ &\quad \times \left. \left( \frac{1}{\gamma^{-2} + (\Psi_f - \Theta)^2} - \frac{1}{\gamma_*^{-2} + (\Psi_f - \Theta)^2} \right) \right\rangle \\ &\quad \times \exp \left( \frac{i\omega}{2} \sum_k \left( \gamma_*^2 + (\Psi_k - \Theta)^2 \right) \tau_k \right) \Bigg], \end{aligned} \quad (22)$$

describing the transition radiation spectral-angular distribution.

By analogy with previous section the averaging in (22) is applied within the frame of dipole approximation. The result of averaging can be presented as

$$\begin{aligned} \omega \frac{dN^{\text{tr}}}{d\omega d^2\Theta} &\approx 2 \frac{e^2}{\pi^2} \left( \frac{1}{\gamma^{-2} + \tilde{\Theta}^2} - \frac{1}{\gamma_*^{-2} + \tilde{\Theta}^2} \right)^2 \\ &\cdot \left[ \tilde{\Theta}^2 \left( 1 - \cos \frac{\omega L}{2} (\gamma_*^{-2} + \tilde{\Theta}^2) \right) + \Psi^2 \left( 1 - \langle \cos \Delta\chi \rangle^{\frac{L}{\tau}} \right) \right. \\ &\quad + \left( \tilde{\Theta}\Psi_i - 2\tilde{\Theta}^2 \left( \frac{1}{\gamma^{-2} + \tilde{\Theta}^2} + \frac{1}{\gamma_*^{-2} + \tilde{\Theta}^2} \right) (\Psi^2 + \tilde{\Theta}\Psi_i) \right) \\ &\quad \left. \times \tilde{\Theta}^2 \left( 1 - \cos \frac{\omega L}{2} (\gamma_*^{-2} + \tilde{\Theta}^2) \right) (1 - \langle \cos \Delta\chi \rangle^{\frac{L}{\tau}}) \right]. \end{aligned} \quad (23)$$

The first term in square brackets in (23) corresponds to the ordinary transition radiation from relativistic electron moving with a constant velocity. The others describe an influence of multiple scattering. The changes in (23) caused by such an influence depend strongly on the orientation angle  $\Psi$  and the target's thickness  $L$ .

To estimate an influence of azimuthal scattering on the total emission properties it is necessary to take into account an interference between the transition radiation and coherent bremsstrahlung. In response to the averaging of the interference term in (5), following from the general expression for total emission amplitude (4) within the frame of dipole approximation, the interference term is reduced to

$$\begin{aligned} \omega \frac{dN^{\text{int}}}{d\omega d^2\Theta} &\approx 2 \frac{e^2}{\pi^2} \frac{1}{\gamma_*^{-2} + \tilde{\Theta}^2} \left( \frac{1}{\gamma^{-2} + \tilde{\Theta}^2} - \frac{1}{\gamma_*^{-2} + \tilde{\Theta}^2} \right) \\ &\times \left[ 2\Psi^2 F_1 - \frac{\gamma_*^{-2} - \tilde{\Theta}^2}{\gamma_*^{-2} + \tilde{\Theta}^2} (\Psi^2 + \tilde{\Theta}\Psi_i)(F_1 - F_2) \right], \\ F_1 &= \frac{\omega_*^2(\tilde{\Theta}) \left( 1 - \langle \cos \Delta\chi \rangle^{\frac{L}{\tau}} \cos \frac{\omega L}{2} (\gamma_*^{-2} + \tilde{\Theta}^2) \right)}{\omega^2 + \omega_*^2(\tilde{\Theta})} \\ &\quad + \frac{\omega \omega_*(\tilde{\Theta}) \langle \cos \Delta\chi \rangle^{\frac{L}{\tau}} \sin \frac{\omega L}{2} (\gamma_*^{-2} + \tilde{\Theta}^2)}{\omega^2 + \omega_*^2(\tilde{\Theta})}, \\ F_2 &= \frac{\omega_*^2(\tilde{\Theta}) \left( \cos \frac{\omega L}{2} (\gamma_*^{-2} + \tilde{\Theta}^2) - \langle \cos \Delta\chi \rangle^{\frac{L}{\tau}} \right)}{\omega^2 \langle \cos \Delta\chi \rangle^2 + \omega_*^2(\tilde{\Theta})} \\ &\quad - \frac{\omega \omega_*(\tilde{\Theta}) \langle \cos \Delta\chi \rangle \sin \frac{\omega L}{2} (\gamma_*^{-2} + \tilde{\Theta}^2)}{\omega^2 \langle \cos \Delta\chi \rangle^2 + \omega_*^2(\tilde{\Theta})}, \end{aligned} \quad (24)$$

where the quantity  $\omega_*(\tilde{\Theta})$  is defined by (13).

The expressions (12), (23) and (24) allow to describe all properties of the dipole emission from relativistic electrons crossing a thin aligned crystal. Let us consider the spectrum of strongly collimated emission ( $\gamma^2 \tilde{\Theta}^2 \ll 1$ ), when a sum of expressions (12), (23) and (24) can be presented in the simple form

$$\begin{aligned} \omega \frac{dN}{d\omega d^2\Theta} &\approx 2 \frac{e^2}{\pi^2} \Psi^2 \left[ (1 - \langle \cos \Delta\chi \rangle) \frac{L}{\tau} \frac{\omega^2}{\omega^2 + \omega_0^2} \gamma_*^4 \right. \\ &\quad \left. + \left( 1 - \langle \cos \Delta\chi \rangle^{\frac{L}{\tau}} \right) (\gamma^2 - \gamma_*^2)^2 + (F_1 + F_2) \gamma_*^2 (\gamma^2 - \gamma_*^2) \right]. \end{aligned} \quad (25)$$

The case being considered is of interest in the context of the anomalous Ter-Mikaelian effect in the bremsstrahlung from relativistic electrons crossing a thin layer of a medium [11]. As for classical Ter-Mikaelian effect, the discussed effect manifests as the dielectric suppression of the bremsstrahlung intensity in low emitted photon energy range  $\omega \leq \gamma\omega_p$ , where the emitted photon phase velocity is changed due to the electromagnetic polarization of medium electrons. But on condition of the emission from thin target under consideration the bremsstrahlung intensity is only partially suppressed in the vicinity of the photon energy  $\omega = \gamma\omega_p$  in contrast with that for the ordinary Ter-Mikaelian suppression manifesting everywhere over the range  $0 < \omega \leq \gamma\omega_p$ .

The anomalous Ter-Mikaelian effect has been studied experimentally and theoretically in the case of relativistic electron bremsstrahlung in a thin amorphous target [7,11]. Here the analogous effect in the coherent bremsstrahlung is analyzed. This effect appearing due to an interference between coherent bremsstrahlung and transition radiation is best realized with the proviso that the contributions of outlined emission mechanisms are comparable. The performed analysis of the expression (25) has shown that such conditions can be realized in the range of large enough orientation angles  $\Psi \gg \Psi_{ch}$ , where the angle of electron azimuthal scattering by a single atomic string  $\Delta\chi$  is small. For simplicity assume that the scattering angle achievable in the single collision of emitting electron with atomic string is small, so that  $\langle \cos \Delta\chi \rangle \simeq 1 - \frac{1}{2}\langle \Delta\chi^2 \rangle$  (in accordance with the corresponding formula in (21) the condition  $\Delta\chi \ll 1$  is fulfilled if  $\Psi^2 \gg \Psi_{ch}^2$ ). In the case under study formula (25) is reduced to more simple one

$$\omega \frac{d^2N}{d\omega d\bar{\theta}} = \frac{4e^2\gamma^2}{\pi} \Psi^2 G(y, z), \quad (26a)$$

$$G = yz \frac{x^4}{(1+x^2)^2 + z^2x^2} + (1 - e^{-yz}) \frac{1}{(1+x^2)^2} + (1 - e^{-yz}) \times \frac{z^2x^2(1 + \cos y(x+x^{-1})) - zx(1+x^2)\sin y(x+x^{-1})}{(1+x^2)^2 + z^2x^2}, \quad (26b)$$

where  $x = \omega/\gamma\omega_p$ ,  $y = \omega_p L/2\gamma$ ,  $z = \gamma\langle \Delta\chi^2 \rangle/\omega_p\bar{\tau}$ . The spectrum distribution by the universal function  $G$  depends strongly on the arguments  $x$ ,  $y$  and  $z$ . As evident from (26) the contribution of coherent bremsstrahlung is suppressed in the range  $x < 1$  or  $\omega < \gamma\omega_p$  due to the normal Ter-Mikaelian effect [1]. As a consequence the relative contribution of transition radiation and the interference term increases in this range of emitted photon energies. The shape of the spectrum is determined by the parameters  $y$  and  $z$ . The parameter  $z$  determines the region of the manifestation of above discussed coherent bremsstrahlung suppression due to azimuthal scattering of emitting electrons by atomic strings. Formally this effect manifests in the frequency range  $\omega < \omega_0$  in response to (17), but in actuality it can be realized with the proviso

that  $\omega_0 > \gamma\omega_p$  because of the Ter-Mikaelian effect of dielectric suppression [1]. It is easy to see that the ratio  $\omega_0/\gamma\omega_p$  is determined by the formula

$$\frac{\omega_0}{\gamma\omega_p} = z \frac{x^2}{1+x^2} \leq z, \quad (27)$$

so that the suppression of coherent bremsstrahlung due to multiple scattering manifests with the constant  $z > 1$  only. In the range  $z \ll 1$  the spectrum is determined in the main by the relationship between transition radiation and coherent bremsstrahlung contributions. This relationship depends on the coefficient  $yz$  (obviously the coefficient  $2yz = \langle \Delta\chi^2 \rangle L/\bar{\tau}$  is equal to mean square of the total azimuthal angle of multiple scattering). In the special case that  $yz \ll 1$  contribution of coherent bremsstrahlung and transition radiation are comparable in the photon energy range  $\omega < \gamma\omega_p$  and the shape of the spectrum takes the form characteristic for the spectrum under condition of anomalous Ter-Mikaelian effect manifestation in bremsstrahlung [7]. The spectral curve is presented in Fig. 3.

In the case of thick enough target that  $yz \gg 1$  the contribution of coherent bremsstrahlung dominates in the frequency range  $\omega > \gamma\omega_p$ . As a consequence, the shape of the spectrum comes close to that for coherent bremsstrahlung suppressed by

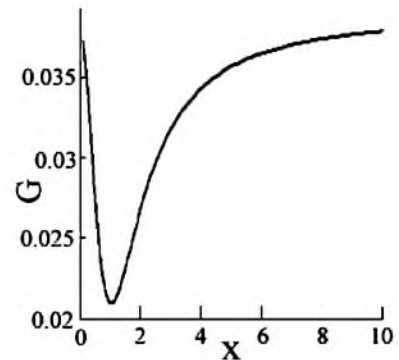


Fig. 3. The spectrum of strongly collimated emission. The presented curves describe the spectral-angular distribution of the emission yield with account of coherent bremsstrahlung, transition radiation and interference term. The function  $G(x, y, z)$  defined by (26) is presented here,  $x = \omega/\gamma\omega_p$ ,  $y = \omega_p L/2\gamma$ ,  $z = \gamma\langle \Delta\chi^2 \rangle/\bar{\tau}\omega_p$ . The curve has been calculated for fixed parameters  $y = 0.1$  and  $z = 0.4$ .

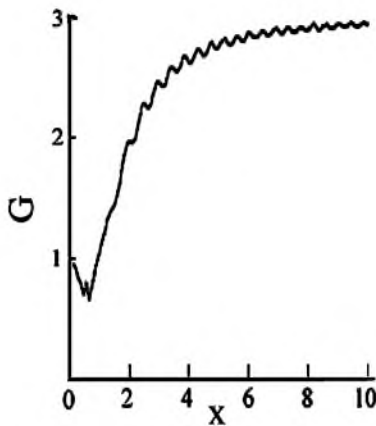


Fig. 4. The same but for  $y = 12$  and  $z = 0.2$ .

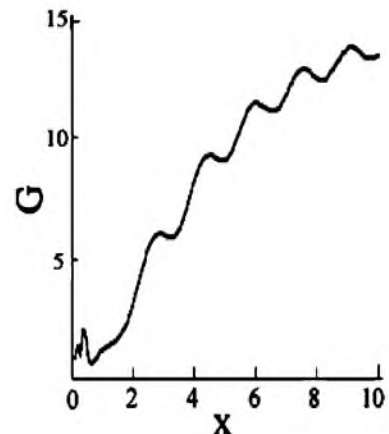


Fig. 6. The same but for  $y = 4$  and  $z = 4$ .

the normal Ter-Mikaelian effect (see the spectral curve presented in Fig. 4).

The emission spectrum is changed substantially in the case  $z \gg 1$ . Suppression of coherent bremsstrahlung due to azimuth multiple scattering and increasing of the role of an interference between transition radiation and coherent bremsstrahlung are the new effects in case in question.

The role of the interference term is demonstrated by Fig. 5, where the spectrum calculated for thin enough target ( $y \ll 1$ ) is presented. Obtained result shows that the interference cannot only suppress completely the Ter-Mikaelian effect manifestation, but it gives rise to strong peak in the emission spectrum as well.

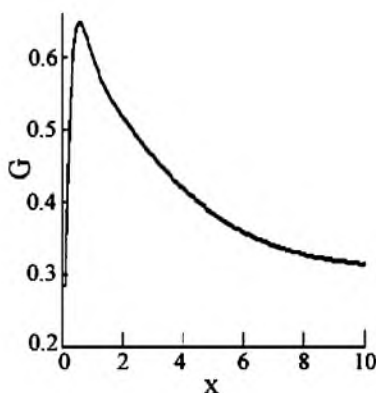


Fig. 5. The same but for  $y = 0.1$  and  $z = 4$ .

In the case  $y > 1$  (since  $L/l_{coh} = y(x + x^{-1}) \geq 2y$ , the interference term in (24) oscillates in the case under consideration) the emission yield is suppressed due to azimuthal multiple scattering in a wide frequency range as it follows from Fig. 6.

Thus, obtained results show that the conventional theory of coherent bremsstrahlung from relativistic electrons crossing a thin aligned crystal is not sufficient for correct description of emission properties in the range of low photon energies where the contributions of coherent bremsstrahlung, transition radiation and interference between these emission mechanisms are comparable and must be taken into account.

## 5. Spectrum of strongly collimated emission beyond the frame of dipole approximation

Returning to the general expression for a total emission amplitude (4), let us consider the characteristics of photons emitted along the atomic string axis and detected by X-ray detector with small angular size  $\Delta\theta \ll \gamma^{-1}$ . Such conditions correspond to the experiment [10]. The expression (4) may be simplified very essentially on condition under consideration because of the important property of a fast charged particle coherent scattering by atomic string  $\Psi_k^2 = \Psi_{k-1}^2 = \Psi^2$ . The following from (4) expression

$$\begin{aligned} \mathbf{A}_n = & \frac{e}{\pi} \left[ \left( \frac{1}{\gamma^2 + \Psi^2} - \frac{1}{\gamma_*^2 + \Psi^2} \right) \right. \\ & \times \left( \Psi_i - \Psi_f \exp \left( \frac{i\omega}{2} (\gamma_*^{-2} + \Psi^2) \sum_k \tau_k \right) \right) \\ & \left. - \sum_k \frac{\Psi_k - \Psi_{k-1}}{\gamma_*^{-2} + \Psi^2} \exp \left( \frac{i\omega}{2} (\gamma_*^{-2} + \Psi^2) \sum_{j \leq k} \tau_j \right) \right], \end{aligned} \quad (28)$$

allows to calculate the emission spectral-angular distribution without complementary approximations. For example, the contribution of coherent bremsstrahlung is described by the formula

$$\omega \frac{dN^{cb}}{d\omega d^2\Theta} = \frac{2e^2\Psi^2}{\pi^2} \frac{1 - \langle \cos \Delta\chi \rangle}{(\gamma_*^{-2} + \Psi^2)^2} \frac{\omega^2}{\omega^2 + \omega_*^2(\Psi)} \frac{L}{\tau}, \quad (29)$$

where the quantity  $\omega_*(\Psi)$  is defined by the formula (13) with a precision of  $\tilde{\Theta} \rightarrow \Psi$ .

Comparison of the exact result (29) with dipole spectral-angular distribution (12) shows that the main characteristics of the collimated dipole coherent bremsstrahlung (the form of spectral distribution and the magnitude of this distribution in the frequency range where it is saturated) are preserved for the emission beyond the frame of dipole approximation.

The contribution of transition radiation, described by the formula

$$\begin{aligned} \omega \frac{dN^{tr}}{d\omega d^2\Theta} = & \frac{2e^2\Psi^2}{\pi^2} \left( \frac{1}{\gamma^2 + \Psi^2} - \frac{1}{\gamma_*^2 + \Psi^2} \right)^2 \\ & \times \left[ 1 - \langle \cos \Delta\chi \rangle^{\frac{L}{\tau}} \cos \frac{\omega L}{2} (\gamma_*^{-2} + \Psi^2) \right], \end{aligned} \quad (30)$$

is not proportional to the target's thickness  $L$  in contrast with (29). The most interesting result following from (30) consists in the suppression of an interference between transition radiation waves emitted from *in* and *out*-surfaces of the target due to emitting particle multiple scattering. Such an effect is manifested for large enough thickness of the target, when the condition opposite to (26) is fulfilled. On the other hand, the yield (30) is

not proportional to  $L$  in the case of thin enough target when the condition (26) is fulfilled.

This difference between (30) and the items in the formula (23) describing an influence of multiple scattering of emitting electrons is caused by non-axial collimation of the emission (30) relative to electron beam axis.

Formulae (29) and (30) must be supplemented by the expression

$$\begin{aligned} \omega \frac{dN^{int}}{d\omega d^2\Theta} = & \frac{4e^2\Psi^2}{\pi^2} \frac{1}{\gamma_*^{-2} + \Psi^2} \left( \frac{1}{\gamma^2 + \Psi^2} - \frac{1}{\gamma_*^2 + \Psi^2} \right) \\ & \times \frac{\omega_*^2(\Psi)}{\omega^2 + \omega_*^2(\Psi)} \left[ 1 - \langle \cos \Delta\chi \rangle^{\frac{L}{\tau}} \cos \frac{\omega L}{2} (\gamma_*^{-2} + \Psi^2) \right. \\ & \left. + \frac{\omega}{2\omega_*} (1 + \langle \cos \Delta\chi \rangle) \langle \cos \Delta\chi \rangle^{\frac{L}{\tau}} \sin \frac{\omega L}{2} (\gamma_*^{-2} + \Psi^2) \right], \end{aligned} \quad (31)$$

describing the contribution of an interference term to total emission yield. Like transition radiation yield, the contribution (31) is not proportional to  $L$ , therefore the coherent bremsstrahlung contribution dominates for thick enough targets.

Let us concentrate attention in the coherent bremsstrahlung from above-barrier fraction of an electron beam crossing the crystalline target along a string axis to estimate the possibility to create an effective X-ray source based on such a kind of emission mechanism. Using the distribution function (20) for emitting electrons one can obtain the following expression for strongly collimated emission spectrum

$$\begin{aligned} \omega \frac{\overline{dN^{cb}}}{d\omega d^2\Theta} = & \frac{2}{\Psi_s^2} \int_0^\infty d\Psi \Psi \left( \frac{\omega}{L} \frac{dN^{cb}}{d\omega d^2\Theta} \right) \\ & \times \left[ E_1 \left( \frac{\Psi^2}{\Psi_0^2 + \Psi_s^2 L} \right) - E_2 \left( \frac{\Psi^2}{\Psi_0^2} \right) \right], \end{aligned} \quad (32)$$

where the function  $\omega dN^{cb}/d\omega d^2\Theta$  is determined by (29).

Unlike the formula (21), the result (30) can be used for comparison with experimental data presented in [10]. The function  $\omega dN^{cb}/d\omega d^2\Theta$ , calculated by (32) for Si(110) crystal with fixed thickness and different electron beam energies, is presented in Fig. 7. In accordance with presented

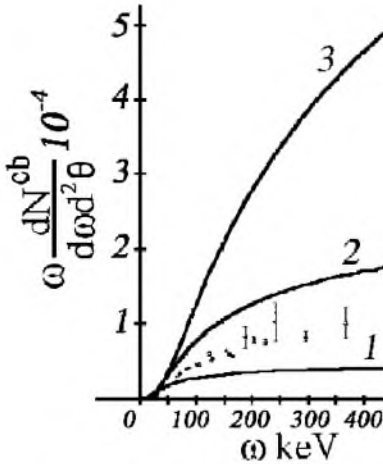


Fig. 7. The spectrum of strongly collimated coherent bremsstrahlung. The presented curves have been calculated by (33) for  $Si(110)$ ,  $\Psi_0 = 0.25 \times 10^{-3}$  rad,  $L = 0.523$  mm. The curves 1–3 correspond to the electron energies 500, 1000 and 2000 MeV, respectively.

curves the emission yield increases essentially when increasing of electron beam energy, but this process is attended by the widening of the photon energy range. Where the discussed suppression effect takes place.

The curve 1 has been calculated for experimental conditions [10]. The theory and data correspond to each other with an accuracy of about 20–30% within the photon energy range  $30 \text{ keV} < \omega < 150 \text{ keV}$ , but the discrepancy increases in the range  $150 \text{ keV} < \omega < 360 \text{ keV}$ , where the calculated emission density is saturated in contrast with obtained data showing the continuing growth of the emission density (it should be noted that statistical errors in the experiment [10] were large in this range). Such a discrepancy may be connected with the contribution of channelling particle emission in small photon energy range due to incoherent scattering processes.

## 6. Landau–Pomeranchuk–Migdal effect in the coherent bremsstrahlung

As indicated above, the spectrum of strongly collimated coherent bremsstrahlung from relativistic electron, crossing an aligned crystal, is sup-

pressed in a small frequency range due to the saturation of emitting particle scattering angle achievable in the process of coherent azimuthal scattering by atomic string's potential. This effect takes place independently on the emitting electron energy and further more the form of the spectrum is the same for both dipole and non-dipole emission processes.

The properties of non-collimated coherent bremsstrahlung are less well understood. In accordance with [3] and results presented above the dipole coherent bremsstrahlung spectrum is proportional to  $\omega$  in the small frequency range, where the discussed suppression effect takes place. On the other hand an analysis of non-collimated coherent bremsstrahlung from electrons with high enough energy, when the emission process is essentially non-dipole, has shown [3] the suppression of coherent bremsstrahlung due to LPM-effect (as this takes place the spectrum is proportional to  $\sqrt{\omega}$  [3]). It is clear that in general case the spectrum of coherent bremsstrahlung in small photon energy range is formed by two mentioned effects. To consider the relation between contributions of these effects to coherent bremsstrahlung spectrum formation let us start from the most general expression for emission spectral-angular distribution [1,6]

$$\omega \frac{dN}{d\omega d\Omega} = \frac{e^2 \omega^2}{4\pi^2} \left\langle \left| \int_{-\infty}^{\infty} dt [\mathbf{n} \mathbf{V}_t] e^{i\omega(t - \mathbf{n}\mathbf{r}_t)} \right|^2 \right\rangle, \quad (33)$$

describing the bremsstrahlung properties within the frame of classical electrodynamics, here  $\mathbf{r}_t = \mathbf{r}(t)$  is the emitting particle trajectory,  $\mathbf{V}_t = \frac{d}{dt} \mathbf{r}_t$ ,  $\varepsilon = 1 - \omega_p^2/\omega^2$ ,  $\mathbf{n}$  is the unit vector to the direction of emitted photon propagation. Integrating (33) over observation angles one can obtain from (33) the following expression for the spectral distribution of emission intensity [2]:

$$\omega \frac{dN}{d\omega d\Omega} = \frac{e^2 \omega}{\pi} \left\langle \int_0^{\infty} d\tau \frac{\mathbf{r}_{t+\tau} - 1/\varepsilon}{|\mathbf{r}_{t+\tau} - \mathbf{r}_t|} [\sin \omega(\tau + \sqrt{\varepsilon}|\mathbf{r}_{t+\tau} - \mathbf{r}_t|) - \sin \omega(\tau - \sqrt{\varepsilon}|\mathbf{r}_{t+\tau} - \mathbf{r}_t|)] \right\rangle. \quad (34)$$

The expression (34) is valid with the proviso that the thickness of the target exceeds essentially the

emission formation length. Using approximations (1a) and (1b) for the emitting electron velocity  $\mathbf{V}_t$ , one can reduce (34) to more simple formula

$$\omega \frac{dN}{dt d\omega} = -\frac{e^2 \omega}{\pi} \left\langle \int_0^\infty \frac{dt}{t} [\gamma_*^{-2} + \Psi^2 - \Psi^2 \cos \Delta\chi_t] \right. \\ \times \left[ \sin(2\omega t) - \sin\left(\frac{\omega}{2}(\gamma_*^{-2} + \Psi^2)t\right) \right. \\ \left. \left. - \frac{\omega \Psi^2}{t} \int_0^t d\tau (t-\tau) \cos \Delta\chi_\tau \right] \right\rangle, \quad (35)$$

which will be used for further analysis.

Averaging in (35) can be performed analytically in the case of small azimuthal scattering angles  $\Delta\chi \ll 1$  [3]. To perform a qualitative analysis in the general case we use the Landau–Pomeranchuk approach [12], replacing the function  $\cos \Delta\chi$  in (35) by the averaged one  $\overline{\cos \Delta\chi_t} = \int_0^{2\pi} d\Delta\chi_t \times \cos(\Delta\chi_t) f(t, \Delta\chi_t)$ , where the distribution function  $f(t, \Delta\chi_t) = (2\pi)^{-1} \sum_k \exp(i k \Delta\chi_t - \alpha_k t)$  is presented, for example in [2]. Obviously

$$\overline{\cos \Delta\chi_t} = \exp(-\alpha_1 t), \\ \alpha_1 = \frac{1 - \langle \cos \Delta\chi \rangle}{\bar{\tau}}. \quad (36)$$

Substituting (36) into (37), one can reduce this formula to simple one

$$\omega \frac{dN}{dt d\omega} = \frac{e^2 \Psi^2 \omega}{\pi} \left\{ \int_0^\infty \frac{dt}{t} (1 - e^{-t}) \sin \frac{\omega}{\omega_*(\Psi)} \right. \\ \times \left( t - \frac{2\gamma_*^2 \Psi^2}{1 + \gamma_*^2 \Psi^2} \frac{t - 1 + e^{-t}}{t} \right) \\ - \frac{\pi}{2} \frac{1}{\gamma_*^2 \Psi^2} \left[ 1 - \frac{2}{\pi} \int_0^\infty \frac{dt}{t} \sin \frac{\omega}{\omega_*(\Psi)} \right. \\ \times \left. \left( t - \frac{2\gamma_*^2 \Psi^2}{1 + \gamma_*^2 \Psi^2} \frac{t - 1 + e^{-t}}{t} \right) \right] \right\}. \quad (37)$$

First of all let us consider the spectrum (37) in the limit  $\omega \ll \omega_*(\Psi)$ . It can easily be shown that the corresponding limit of this formula

$$\omega \frac{dN}{dt d\omega} \simeq \frac{2e^2 \gamma_*^2 \Psi^2}{\pi(1 + \gamma_*^2 \Psi^2)} \frac{1 - \langle \cos \Delta\chi \rangle}{\bar{\tau}} \frac{\pi}{2} \frac{\omega}{\omega_*(\Psi)} \\ = \frac{2e^2}{\pi} \gamma_*^2 \Psi^2 \frac{1 - \langle \cos \Delta\chi \rangle}{\bar{\tau}} \frac{\pi}{2} \frac{\omega}{\omega_0}, \quad (38)$$

coincides with the dipole result (17) and (18).

It is very important that the form of the spectrum (38) (proportion to  $\omega$ ) does not depend on the emitting electron energy. In other words, the LPM-effect is not manifested within the range of emitted photon energies  $\omega \ll \omega_*(\Psi)$  and the coherent bremsstrahlung spectrum is determined in this range by the effect of emission suppression due to discussed above limitation on a value of emitting electron scattering angle achievable in the process of coherent azimuthal scattering by string's potential.

In the range of high emitted photon energies  $\omega \gg \omega_*(\Psi)$  effective values of  $t$  in integrals (37) are small and, therefore, the formula (38) can be reduced to the following one:

$$\omega \frac{dN}{dt d\omega} \simeq \frac{e^2 \Psi^2 \omega}{\pi} \\ \times \left\{ \frac{4\alpha_1 \gamma_*^2}{\omega} \int_0^\infty dt \sin \left( 2t + \frac{\omega_L}{\omega} t^2 \right) - \frac{\pi}{2} \frac{1}{\gamma_*^2 \Psi^2} \right. \\ \times \left[ 1 - \frac{2}{\pi} \int_0^\infty \frac{dt}{t} \sin \left( 2t + \frac{\omega_L}{\omega} t^2 \right) \right] \left. \right\}, \quad (39)$$

where  $\omega_L = \frac{8}{3} \gamma_*^4 \Psi^2 (1 - \langle \cos \Delta\chi \rangle) / \bar{\tau}$  is the characteristic energy of Landau–Pomeranchuk–Migdal effect manifestation in the coherent bremsstrahlung [3].

As can be seen from (39), the coherent bremsstrahlung is determined within the range  $\omega \ll \omega_L$  by the LPM-effect

$$\omega \frac{dN}{dt d\omega} \simeq \frac{2e^2 \Psi^2 \gamma_*^2}{\pi} \frac{1 - \langle \cos \Delta\chi \rangle}{\bar{\tau}} \sqrt{\frac{\pi}{2} \frac{\omega}{\omega_L}}. \quad (40)$$

The formula (40) describes the emission suppression relative to asymptotic result

$$\omega \frac{dN}{dt d\omega} \simeq \frac{2e^2 \Psi^2 \gamma_*^2}{\pi} \frac{1 - \langle \cos \Delta\chi \rangle}{\bar{\tau}}, \quad (41)$$

following from (39) in the limit  $\omega_L/\omega \rightarrow 0$  (to obtain (41) from (39) it is necessary to use the formula  $\lim(\int_0^\infty dx e^{-\beta x} \sin x)|_{\beta \rightarrow 0} = 1$ ). It should be noted that the result (41) differs by only a factor 3/2 from the corresponding limit (18) of the dipole spectrum (17).

The two spectra (38) and (40) diverged considerably. Obviously, the Landau–Pomeranchuk–Migdal spectrum (40) can be realized with the

proviso that  $\omega_L \gg \omega_*(\Psi)$  only. Such a condition can be presented as

$$\frac{\omega_L}{\omega_*(\Psi)} = \frac{4}{3} \gamma_*^2 \Psi^2 (1 + \gamma_*^2 \Psi^2) \gg 1. \quad (42)$$

Thus, the coherent bremsstrahlung spectrum at the indicated conditions has three different sections. In the first of them ( $\omega < \omega_*(\Psi)$ ), the spectrum is described by the formula (38). The emission yield is strongly suppressed in this range due to the limitation on the value of emitting particle scattering angle. Within the range  $\omega_*(\Psi) < \omega < \omega_L$  the emission suppression due to LPM-effect is realized. The field of existence of this effect vanishes if  $\gamma^2 \Psi^2 \ll 1$  in accordance with (42). Physical meaning of the condition  $\gamma^2 \Psi^2 \ll 1$  is very simple. As is evident from (14) this condition implies that the emission process is dipole and it is reasonable that LPM-effect does not appear. Finally, the coherent bremsstrahlung spectrum peaks in the range  $\omega > \omega_L$ .

## 7. Conclusions

In accordance with performed analysis, the spectrum of coherent bremsstrahlung from relativistic electrons crossing an aligned crystal near parallel to atomic string axis is determined in the low photon energy range by the coherent azimuthal multiple scattering of emitting electrons on a set of atomic strings.

An inherent properties of such a scattering process consists in the limitation on the value of scattering angle. This effect causes the strong suppression of the dipole coherent bremsstrahlung yield from a crystalline target as compared to the coherent bremsstrahlung on a single atomic string. As this takes place, the spectrum of strongly collimated emission is proportional to  $\omega^2$  in small frequency range, but the spectrum of weakly collimated emission is proportional to  $\omega$  within the range where the discussed suppression effect is manifested.

Transition radiation and its interference with the coherent bremsstrahlung make on essential contribution to total emission yield from a thin target. Among other things this effect can change strongly the manifestation of both the effect of

coherent bremsstrahlung suppression due to the limitation of the azimuthal multiple scattering angle and the Ter-Mikaelian effect of coherent bremsstrahlung suppression due to the polarization of medium electrons. The spectrum of coherent bremsstrahlung strongly collimated along the atomic string axis is proportional to  $\omega^2$  in small frequency range independently on the energy of emitting electrons.

The spectrum of non-collimated coherent bremsstrahlung depends strongly in the emitting electron energy. Within the range of small enough energies, where the condition  $\gamma \Psi < 1$  is fulfilled, the spectrum is proportional to  $\omega$  in the range  $\omega < \omega_*(\Psi)$  (see formula (13)) and is saturated in the range  $\omega > \omega_*(\Psi)$ . LPM-effect does not manifest under such conditions. In the range  $\gamma \Psi \gg 1$  the spectral segment  $\omega_*(\phi) < \omega < \omega_L(\Psi)$  (see (39) and (40)) appears, where the spectrum is proportional to  $\sqrt{\omega}$  in accordance with LPM-effect.

## Acknowledgements

This work was supported by the Russian Foundation of Basic Research (grant 02-02-16941), Program Universities of Russia (grants 02.01.012, 02.01.018) and Federal-Regional Program for the support of science researches (grant FRP-9-03). One of the authors (P.Zh.) is grateful to Russian Ministry of Education for financial support of young scientists (grant A 03-2.9-551) and to both Russian Ministry of Education and Administration of Belgorod Region for financial support (grant GM-06-03).

## References

- [1] M. Ter-Mikaelian, High Energy Electromagnetic Processes in Condensed Media, Wiley, New-York, 1972.
- [2] A.I. Akhiezer, N.F. Shulga, High Energy Electrodynamics in Matter, Gordon and Breach, London, 1996.
- [3] N.V. Laskin, A.S. Mazmanishvili, N.N. Nasonov, N.F. Shulga, Sov. Phys. JETP 62 (1985) 438.
- [4] O. Pedersen, J.U. Andersen, E. Bonderup, Nucl. Instr. and Meth. B 13 (1986) 27.
- [5] N.N. Nasonov, N.F. Shulga, Ukr. Fiz. Zhurn. 27 (1982) 789.

- [6] L.D. Landau, E.M. Lifshitz, *The Classical Theory of Field*, Pergamon Press, Oxford, 1980.
- [7] N.N. Nasonov, *Nucl. Instr. and Meth. B* 173 (2001) 203.
- [8] S.M. Rytov, *Vvedenie v statisticheskiju radiofiziku*, Nauka, Moscow, 1976.
- [9] M.L. Ter-Mikaelian, *Dokl. Akad. Nauk USSR* 94 (1954) 1033.
- [10] B.N. Kalinin, G.A. Naumenko, D.V. Padalko, A.P. Potylitsin, I.E. Vnukov, *Nucl. Instr. and Meth. B* 173 (2001) 253.
- [11] U. Arkatov, S. Blazhevich, G. Bochek, E. Gavrilichev, A. Grinenko, V. Kulibaba, N. Maslov, N. Nasonov, V. Pirogov, Y. Virchenko, *Phys. Lett. A* 219 (1996) 355.
- [12] L.D. Landau, I.Ya. Pomeranchuk, *Dokl. Akad. Nauk SSSR* 92 (1953) 735.